Intramolecular Diffusion-Controlled Reactions in Polymers in the Optimized Rouse–Zimm Approach. 1. The Effects of Chain Stiffness, Reactive Site Positions, and Site Numbers

Angelo Perico* and Monica Beggiato

Centro di Studi Chimico-Fisici di Macromolecole Sintetiche e Naturali, CNR, Istituto di Chimica Industriale, Università di Genova, Corso Europa 30, 16132 Genova, Italy.
Received March 3, 1989; Revised Manuscript Received May 25, 1989

ABSTRACT: The Wilemski–Fixman approach to diffusion-controlled intramolecular reactions in polymer solutions is extended to the optimized Rouse–Zimm (ORZ) hierarchy of dynamic models. The effect of chain stiffness is treated by using the ORZ approximation of the freely rotating chain in the entire range between Gaussian chains and rods. For two reactive sites in the interior of the chain, the pure dynamic effect of the length of the lateral tails on the rate constant is considered and found to be dependent on the capture radius. The case of evenly spaced catalytic sites with a central reactive group is exactly solved and the results are compared with the simple hypothesis of the reaction additivity.

Introduction

Fast intramolecular reactions in polymers are a fascinating field, deeply related to polymer dynamics on different length scales and to selective intramolecular reactivity, both being of importance in technology and biology.

In a series of three classical papers in 1973–1974, Wilemski and Fixman (WF) gave a sound theoretical foundation to fast intramolecular reactions.[1-3] As a result a large body of work was done to develop a theoretical predictions and suitable experimental techniques.

In 1984, Cuniberti and Perico presented a comprehensive review of the experimental and theoretical work performed during the past 10 years.[4] Exciplex and especially pyrenil excimer formation were successfully studied as examples of fast intramolecular reactions.[5,6] Detailed theoretical predictions were given for end-to-end cyclization dynamics in flexible Gaussian chains.[7] Steady-state and or transient fluorescence measurements on pyrenyl-termined poly(ethylene oxide) and polystyrene under Θ conditions showed a good agreement with the predicted molecular weight dependences.[5,8,9] The specific conformational features of the polymer were reasonably described in terms of Kuhn lengths and some partial draining effects emerged. Approximate introduction of excluded-volume interaction and screened hydrodynamic and excluded-volume interactions could qualitatively explain experiments in good solvents and dilute labeled chains in concentrated solutions.[8-14] Experiments on polymers containing evenly spaced pyrenyl groups were interpreted by using a rough approximation to the WF theory of diffusion-controlled reactions (DCR). This approximation is based on reaction additivity and on asymptotic ($n \rightarrow \infty$) behavior for each individual rate constant.[11] Both approximations were unjustified (the DCR theory is formally nonadditive and intramolecular distances are not long enough) but, unexpectedly, enabled a consistent interpretation of the large body of experimental results.[11,12]

So we would like to theoretically answer several open questions in this series of papers. The first question we want to address is how to overcome the use of the Gaussian chain as a basic model, taking advantage of the progress of the polymer dynamic theory. First we will summarize the WF theory showing its validity in the optimized Rouse–Zimm (ORZ)[15] approximation to the generalized diffusion equation. This will enable us to consider more accurately the conformational structure of every specific polymer thus avoiding the parametrization of chain stiffness in terms of segment length. For instance, this parametrization may be too restrictive to face reactions on biological macromolecules built of different units and of finite length. In addition, in pyrenyl excimer formation experiments, the fluorescence lifetime limits the distance between the reactive groups, which can be considered. As a consequence the rate constant is more sensitive to the accurate description of the conformational details of the chain.

As a first application of the ORZ hierarchy of dynamic models, the ORZ approximation to the freely rotating model is used in this paper to describe the effect of the mean persistence length of the chain.

A second question is related to the calculation of a specific dynamic effect: the effect of the tails on the rate constant between two reactive groups in the interior of the chain.

Finally, the case of a reactive site in a chain with evenly spaced catalytic sites is solved exactly in order to discuss the approximations of additivity and asymptoticity.

In forthcoming papers the reaction rate constants for intramolecular reactions for rotational isomeric state models of real polymer chains will be presented first, and, finally, an extensive comparison with the experimental results, obtained by pyrenyl excimer formation technique, will be presented.

The ORZ-DCR Theory for Catalytic Reactions

Consider a catalytic reaction between a reactive group in position i_r and n_c catalytic groups in position i_p, $p = 1, ..., n_c$ (see Figure 1a). The WF derivation of the reaction rate constant between the reaction group in i_r and the n_c catalytic groups is herein summarized, avoiding the restriction to Gaussian chain models. The reaction is described by adding a nonconservative sink term to the Smoluchowski generalized diffusion equation in the chain full configuration space.

$$\partial\psi/\partial t + G\psi = -kS\psi \tag{1}$$

The chain is described as a collection of n units (monomers or beads) of coordinates $\{R_i; i = 0, 1, ..., n-1\}$ connected by bonds (or effective bonds) of root mean square length l; $\psi(\{\mathbf{R}_i\},t)$ is the distribution function at time t in

0024-9297/90/2223-0797$02.50/0

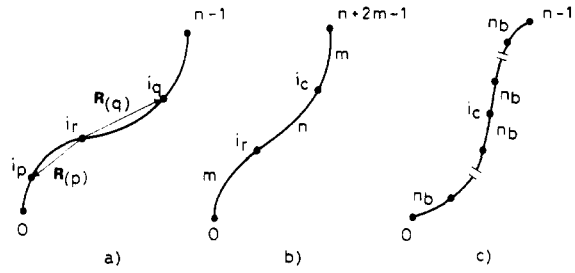

Figure 1. Configuration schemes for the intramolecular reactions: (a) general scheme; (b) one reactive group in position i_r and one catalytic group, in position i_c, with two equal tails m beads long; $i_r = m$; $i_c = n + m - 1$; total number of beads $n + 2m$; (c) the evenly spaced reaction configuration, a reactive group in the center of the chain with n_c catalytic sites with a spacing n_b and $n_b n_c + 1 = n$.

the configuration space $\{\mathbf{R}_i\}$ and G is the diffusion operator, which includes the mean field intramolecular potential $V(\{\mathbf{R}_i\})$.

The reactions are characterized by an identical intrinsic rate constant k and the sink operator S defines the region of space where the reaction can occur

$$S = \sum_{p=1}^{n_c} S_p(\mathbf{R}_{(p)}) \tag{2}$$

with $\mathbf{R}_{(p)}$ the distance of the reactive group i_r from the catalytic group i_p.

Let us formally introduce the Green function of the generalized diffusion equation, $W_2(\{\mathbf{R}_i\},t;\{\mathbf{R}_i^0\},t_0)$, or joint probability to find a configuration $\{\mathbf{R}_i^0\}$ at the initial time t_0 and a configuration $\{\mathbf{R}_i\}$ at time t. Then the solution of eq 1, treating the term on the right-hand side as an unhomogeneous term, is given by[16]

$$\psi(\{\mathbf{R}_i\},t) = \psi_{eq}(\{\mathbf{R}_i\}) - k \times \int_0^t dt_0 \int d\{\mathbf{R}_i^0\}\, W_2(\{\mathbf{R}_i\},t-t_0;\{\mathbf{R}_i^0\},t_0) S(\{\mathbf{R}_i^0\}) \psi(\{\mathbf{R}_i^0\},t_0) \tag{3}$$

with the assumption that at the initial time $t_0 = 0$ the polymer distribution function is at equilibrium, $\psi_{eq}(\{\mathbf{R}_i\})$. By introducing the "closure approximation"[3] in the integral to the right-hand side of eq 3

$$S(\{\mathbf{R}_i^0\})\psi(\{\mathbf{R}_i^0\},t_0) \simeq S(\{\mathbf{R}_i^0\})\psi_{eq}(\{\mathbf{R}_i^0\})C(t)/C_{eq} \tag{4}$$

with

$$C(t) = \int d\{\mathbf{R}_i\}\, S(\{\mathbf{R}_i\})\psi(\{\mathbf{R}_i\},t) \tag{5}$$

and $C_{eq} \equiv C(0)$ and integrating eq 3 after premultiplication by $S(\{\mathbf{R}_i\})$ we get the convolution equation for $C(t)$

$$C(t) = C_{eq} - (k/C_{eq}) \int_0^t D(t - t_0) C(t_0)\, dt_0 \tag{6}$$

Here $D(t - t_0)$ is the reduced Green function

$$D(t - t_0) = \int d\{\mathbf{R}_i\}\, d\{\mathbf{R}_i^0\}\, W_2(\{\mathbf{R}_i\},t-t_0;\{\mathbf{R}_i^0\},t_0) S(\{\mathbf{R}_i\}) S(\{\mathbf{R}_i^0\}) \tag{7}$$

The C_{eq} and $C(t)$ are the equilibrium and time t concentrations of catalytic groups near the still-active reactive group. The "closure approximation" has been extensively discussed and found to be fairly accurate.[17,18]

The probability of having the reactive group still unreacted at time t

$$\phi(t) = \int \psi(\{\mathbf{R}_i\},t)\, d\{\mathbf{R}_i\} \tag{8}$$

is governed by the equation

$$\partial\phi/\partial t = -kC(t) \tag{9}$$

obtained by integration of (1) using the conservative properties of the diffusion operator. By Laplace transform techniques, the solution of eq 6 and 9 is found to be

$$\phi(t) = \sum_i \phi_i \exp(-\delta_i t) \tag{10}$$

with $-\delta_i$ and ϕ_i the poles of the Laplace transform $\hat{\phi}(s)$ of $\phi(t)$ and the residue at the pole $-\delta_i$:

$$\delta_i = kC_{eq}/[1 + (k/C_{eq})\hat{H}(-\delta_i)] \tag{11}$$

with

$$H(t) = D(t) - C_{eq}^2 \tag{12}$$

and $\lim_{t\to\infty} H(t) = 0$.

All the $\{\delta_i,\phi_i\}$ couples can be calculated by carefully taking into account the singularities of $\hat{D}(s)$. However, it may be shown[3] that the first couple $\{\delta_1,\phi_1\}$ describes the main part of the reactive process according to the approximation $\phi_1 \simeq 1$ and

$$\phi(t) \simeq \exp(-\delta_1 t) \tag{13}$$

Therefore, the first-order rate constant of the catalytic process is simply

$$k_1 = -\phi^{-1}\frac{d\phi}{dt}\bigg|_{t=0} \simeq \delta_1 \tag{14}$$

In the limit of complete diffusion control or a very fast intrinsic reaction rate ($k \to \infty$) we get from (11):

$$k_1^D = \left\{\int_0^\infty \frac{D(t) - C_{eq}^2}{C_{eq}^2} \exp(k_1^D t)\, dt\right\}^{-1} \tag{15}$$

The central quantity to be calculated is the reduced Green function $D(t)$, which is a functional quadratic in the sink function and linear in the Green function W_2. Let us introduce a δ representation of the sink function

$$S(\{\mathbf{R}_i\}) = \sum_{p=1}^{n_c} \int d\mathbf{u}\, \delta(\mathbf{u} - \mathbf{R}_{(p)}) S(\mathbf{u}) \tag{16}$$

where, we have also assumed, for simplicity's sake, that the catalytic groups are identical. Therefore the index p on $S_p(\mathbf{u})$ can be dropped. With this assumption $S(\mathbf{u})$ is now a function of the variable $\mathbf{u}$ alone and of the general structure of the sink, characterizing the catalytic reaction, to be discussed below. Putting (16) into (7) and taking the Fourier representations of the δ functions we get

$$D(t) = \int d\mathbf{u}_1\, S(\mathbf{u}_1) \int d\mathbf{u}_2\, S(\mathbf{u}_2) \int \frac{d^3k_1}{(2\pi)^3} \int \frac{d^3k_2}{(2\pi)^3} \times \exp\{i(\mathbf{k}_1\cdot\mathbf{u}_1 + \mathbf{k}_2\cdot\mathbf{u}_2)\} F(\mathbf{k}_1,\mathbf{k}_2,t) \tag{17}$$

with $F(\mathbf{k}_1,\mathbf{k}_2,t)$ the generalized dynamic structure factor

$$F(\mathbf{k}_1,\mathbf{k}_2,t) = \sum_{p,q=1}^{n_c} \langle \exp\{-i\mathbf{k}_1\cdot\mathbf{R}_{(p)} - i\mathbf{k}_2\mathbf{R}^0_{(q)}\}\rangle \tag{18}$$

The average $\langle\ \rangle$ is taken with the two time Green function W_2. This quantity W_2 is easily calculated by the Wang–Uhlenbeck method[19] for any model of the ORZ hierarchy obeying the Langevin equation[20]

$$\frac{\partial}{\partial t}\mathbf{R}_i(t) + \sigma\sum_{j=0}^{n-1}(\mathbf{HA})_{ij}\mathbf{R}_j(t) = \mathbf{v}^*_i(t) \tag{19}$$

with

$$\sigma = 3k_B T/l^2\zeta \tag{20}$$

and ζ the bead friction coefficient, describing the time evolution of the bead coordinates under random forces, responsible for the Gaussian random velocity $\mathbf{v}^*_i(t)$, the intramolecular potential $V(\{\mathbf{R}_i\})$, friction forces, and hydrodynamic interactions (between friction forces and flow). The matrix $\mathbf{A}$ of order n is given in terms of the inverse $\mathbf{U}$ of the static bond correlation matrix[21]

$$U^{-1}_{ij} = \langle \mathbf{l}_i \cdot \mathbf{l}_j \rangle / l^2 \tag{21}$$

as

$$\mathbf{A} = \mathbf{M}^{\mathrm{T}} \begin{pmatrix} 0 & 0 \\ 0 & \mathbf{U} \end{pmatrix} \mathbf{M} \tag{22}$$

with the matrix $\mathbf{M}$ of order n given by

$$\mathbf{M} = \begin{bmatrix} \frac{1}{n} & \frac{1}{n} & \frac{1}{n} & \cdot & \cdot \\ -1 & 1 & 0 & 0 & \cdot \\ 0 & -1 & 1 & 0 & \cdot \\ \cdot & \cdot & \cdot & \cdot & \cdot \end{bmatrix} \tag{23}$$

The matrix $\mathbf{H}$ is the hydrodynamic interaction matrix averaged over the polymer configurations

$$H_{ij} = \delta_{ij} + \zeta_r \langle 1/R_{ij} \rangle (1 - \delta_{ij}) \tag{24}$$

with

$$\zeta_r = \zeta / 6\pi\eta_0 l \tag{25}$$

the hydrodynamic interaction strength, with η_0 the solvent viscosity.

Equation 19 is decoupled by diagonalization of matrix $\mathbf{HA}$ via the transformation to normal coordinates $\xi_a(t)$:

$$\mathbf{R}_i(t) = \sum_{a=0}^{n-1} Q_{ia} \xi_a(t) \tag{26}$$

obtaining

$$\left(\frac{\partial}{\partial t} + \sigma\lambda_a \right) \xi_a(t) = \mathbf{v}^*_a(t) \tag{27}$$

with λ_a and $\mathbf{Q}$ the eigenvalues and eigenvector matrix of $\mathbf{HA}$. Equation 27 is solved by standard statistical methods of Gaussian random processes, in terms of the Gaussian bivariate[19,20]

$$W_2(\xi_a(t),\xi_a(0)) = (3/2\pi\langle \xi^2_a \rangle^{3/2}) \exp\{-3|\xi_a(0)|^2/2\langle \xi^2_a \rangle\} \times \{3/2\pi\langle \xi^2_a \rangle [1 - \exp(-2\sigma\lambda_a t)]\}^{3/2} \exp\{-(3/2)|\xi_a(t) - \xi_a(0) \times \exp(-\sigma\lambda_a t)|^2 / [\langle \xi^2_a \rangle [1 - \exp(-2\sigma\lambda_a t)]]\} \tag{28}$$

From this expression the generalized dynamic structure factor $F(\mathbf{k}_1,\mathbf{k}_2,t)$ is easily calculated by Fourier transform properties to obtain

$$F(\mathbf{k}_1,\mathbf{k}_2,t) = \sum_{p,q=1}^{n_c} \exp\{-(1/6)[k^2_1 \langle R^2_{(p)} \rangle + k^2_2 \langle R^2_{(q)} \rangle + 2(\mathbf{k}_1 \cdot \mathbf{k}_2) \langle \mathbf{R}_{(p)}(t) \cdot \mathbf{R}_{(q)}(0) \rangle]\} \tag{29}$$

Introducing this expression in (17) and again using the Fourier transform properties, we obtain the final formal result

$$D(t) = \int d\mathbf{u}_1 \, \mathbf{S}(\mathbf{u}_1) \int d\mathbf{u}_2 \, S(\mathbf{u}_2) \sum_{p,q=1}^{n_c} G_{pq}(\mathbf{u}_1,\mathbf{u}_2,t) \tag{30}$$

with $G_{pq}(\mathbf{u}_1,\mathbf{u}_2,t)$ the bivariate Gaussian distribution function

$$G_{pq}(\mathbf{u}_1,\mathbf{u}_2,t) = [3/2\pi(\langle R^2_{(p)} \rangle)^{1/2}(\langle R^2_{(q)} \rangle)^{1/2}(1 - \rho^2_{(p)(q)}(t))^{1/2}]^3 \times \exp\{-(3/2)[\langle R^2_{(q)} \rangle u^2_1 + \langle R^2_{(p)} \rangle u^2_2 - 2(\langle R^2_{(p)} \rangle \langle R^2_{(q)} \rangle)^{1/2} \times \rho_{(p)(q)}(t) \mathbf{u}_1 \cdot \mathbf{u}_2] / [\langle R^2_{(p)} \rangle \langle R^2_{(q)} \rangle (1 - \rho^2_{(p)(q)}(t))] \tag{31}$$

Here we have introduced the fundamental time correlation function for the vector distances $\mathbf{R}_{(p)}(t)$, $\mathbf{R}_{(q)}(0)$ between the reactive site in position i_r and the catalytic sites in position i_p, i_q (see Figure 1):

$$\rho_{(p)(q)}(t) = \langle \mathbf{R}_{(p)}(t) \cdot \mathbf{R}_{(q)}(0) \rangle / (\langle R^2_{(p)} \rangle)^{1/2}(\langle R^2_{(q)} \rangle)^{1/2} = \equiv [\sum_{a=1}^{n-1} (Q_{(p),a} - Q_{(r),a})(Q_{(q),a} - Q_{(r),a}) \mu^{-1}_a \exp(-\sigma\lambda_a t)] / [\sum_{a=1}^{n-1} (Q_{(p),a} - Q_{(r),a})^2 \mu^{-1}_a]^{1/2} [\sum_{a=1}^{n-1} (Q_{(q),a} - Q_{(r),a})^2 \mu^{-1}_a]^{1/2} \tag{32}$$

(p), (q), and (r) are also used here as a shorthand notation for i_p, i_q, and i_r.

The last equation has been obtained by using (26) and the properties of normal modes with

$$\mu^{-1}_a = \langle \xi^2_a \rangle / l^2 \tag{33}$$

the normalized mean-square length of the normal mode a.

The sink function in (30) remains to be defined: the simpler the sink function, the easier the integrals to be calculated in (30), (11), and (15). Avoiding the simplest δ function, giving a $D(t)$ highly singular in $t = 0$, in the following we will choose the popular unbalanced choice amounting to a δ function for one sink and an Heaviside sink for the other.[3,17] This choice introduces a capture radius R as the reaction parameter in space. Other choices are almost equivalent. The general features of the sink function, together with a few examples, are reported in appendix A.

When this sink is substituted in (30) we obtain

$$D(t) = [(4/3)\pi R^3]^{-1} \sum_{p,q=1}^{n_c} (1/2)\{[(2\pi/3)\langle R^2_{(q)} \rangle]^{-3/2} I(z_{(p)(q)}) + [(2\pi/3)\langle R^2_{(p)} \rangle]^{-3/2} I(z_{(q)(p)})\} \tag{34}$$

and

$$I(z) = \mathrm{erf}\,(z) - (2/\pi^{1/2}) z \exp(-z^2) \tag{35}$$

$$z_{(p)(q)} = \gamma_{(p)}(1 - \rho^2_{(p)(q)}(t))^{-1/2} \tag{36}$$

with

$$\gamma_{(p)} = \gamma_0 (l^2 / \langle R^2_{(p)} \rangle)^{1/2}; \quad \gamma_0 = (3/2)^{1/2} R/l \tag{37}$$

where γ_0 is the adimensional capture strength.

Note that the average in (34), $(1/2)\{\}$, has been introduced to get the correct physical symmetry in $D(t)$ with respect to (p) and (q), lost with the introduction of the unbalanced choice.

With these results for $D(t)$, the diffusion controlled rate constant k_1^{D}, eq 15, becomes

$$\sigma / k_1^{\mathrm{D}} = \int_0^\infty F(\tau) \, d\tau \tag{38}$$

with

$$\tau = \sigma t \tag{39}$$

the adimensional time and

$$F(\tau) = \exp(k_1^{\mathrm{D}}/\sigma)\tau [\sum_{p,q=1}^{n_c} \{\gamma^3_{(q)}[I(z_{(p)(q)}) - I(\gamma_{(p)})] + \gamma^3_{(p)}[I(z_{(q)(p)} - I(\gamma_{(q)}]\}/2[\sum_q \gamma^3_{(q)}][\sum_p I(\gamma_{(p)})] \tag{40}$$

The integral (38) is performed by an iterative numerical quadrature procedure, quickly converging due to the weak dependence on the exponential in front of eq 40. The numerical integration is better performed on the normalized function $F(\tau)/F(0)$, which decays to zero in the large time limit. As this decaying function is strongly nonexponential, quadrature methods on a semiinfinite interval, like the Laguerre–Gauss procedure, are very unreliable. It is preferable to divide the total interval into a properly designed number of subintervals and to apply a Gauss–Legendre quadrature to each subinterval. In addition, due to the enormous variability of $F(\tau)/F(0)$ with the physical parameters (polymer length and structure, capture radius, etc.), it is better to introduce a scaling procedure to remove this variability in order to obtain subintervals approximately independent of the physical parameters. This result is obtained by scaling the time variable by using a good approximation to the integral, $\tau_p/F(0)$, of the normalized function according to

$$\sigma/k_1^{\mathrm{D}} = \tau_p \int_0^\infty \mathrm{d}x\, F(x\tau_p/F(0))/F(0) \qquad (41)$$

thus obtaining an integral on the order of unity. The procedure to derive the aestimation τ_p in the cases of interest in this paper is outlined in Appendix B.

The Stiffness Effect on the Cyclization Rate Constant

The cyclization rate constant is obtained for a reactive and a catalytic group at the two chain terminals. This case is obtained from the general formula (38) with (40) having $n_c = 1$, $i_r = 0$, $i_p = i_q = n - 1$ and

$$\gamma_{(p)} = \gamma = (3/2)^{1/2} R/L \qquad (42)$$

with L^2 the end-to-end mean square distance.

To describe the stiffness of the chain we choose the ORZ approximation to the freely rotating chain model (FRC)[15,22] characterized by a stiffness parameter

$$g = -\cos\theta \qquad (43)$$

with θ the valence angle.

Note that in the ORZ approximation $g = 0$ corresponds to the bead–spring model or Gaussian chain, while $g = 1$ to the rod limit. The proper λ_a, μ_a, and Q for the ORZ-FRC model are calculated according to the procedure outlined elsewhere[22] and used to derive the cyclization rate constant as a function of the polymer length n and stiffness g.

All the calculations reported in this paper were performed in the partial draining case with $\zeta_r = 0.25$, typical of a Θ solution. In Figure 2, the effect of the capture strength on the first order cyclization rate constant is reported for several values of n and $g = 0$. Similar plots are obtained for $g \neq 0$. For a discrete chain the rate constant is linear in γ_0, at small γ_0, and in the limit $R \to 0$ there is no reaction ($k_1^{\mathrm{D}} = 0$). Evidence of this capture strength effect has been found experimentally by intramolecular exciplex formation.[6] Note that this linear behavior in γ_0 is not in contrast with the behavior, found and discussed earlier,[7] of a second-order rate constant $k_1^{\mathrm{D}}/C_{\mathrm{eq}}$ in the asymptotic limit $n \to \infty$ at fixed R.

In Figure 3 the dependence of k_1^{D} on the stiffness g is reported for two values of the capture strength and some values of n. As expected, with increasing stiffness the rate constant k_1^{D} strongly and continuously reduces. In the rod limit a small but nonzero result is obtained as is shown in Figure 4. Obviously the cyclization cannot occur (at small capture strength) in a rigid rod, therefore this result shows the failure of the ORZ model of DCR in the large stiffness range. In fact, in the ORZ approximation to the DCR theory the limiting values for $g = 1$ are the values for a harmonic spring of mean square length equal to the square of the rod length. In contrast, for semiflexible chains, the ORZ-FRC model moderately improves the simple Gaussian model, used earlier in the interpretation of intramolecular excimer experiments.

In the ORZ-FRC model the rate constant is given in terms of the number of bonds $n - 1$ and of a definite

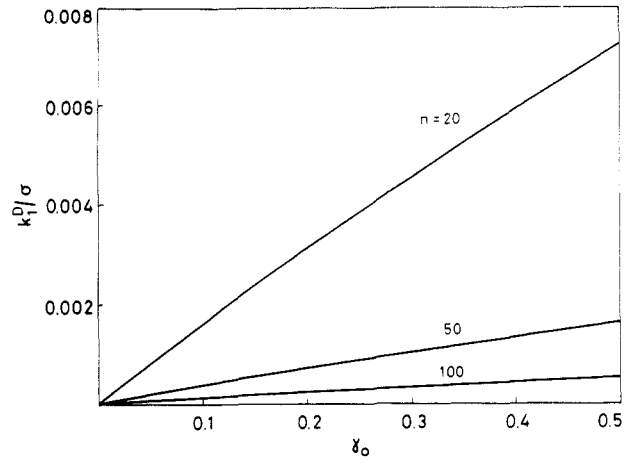

Figure 2. Normalized diffusion-controlled cyclization rate constant k_1^{D}/σ as a function of the capture strength γ_0 for $n = 20$, 50, and 100. Gaussian chain.

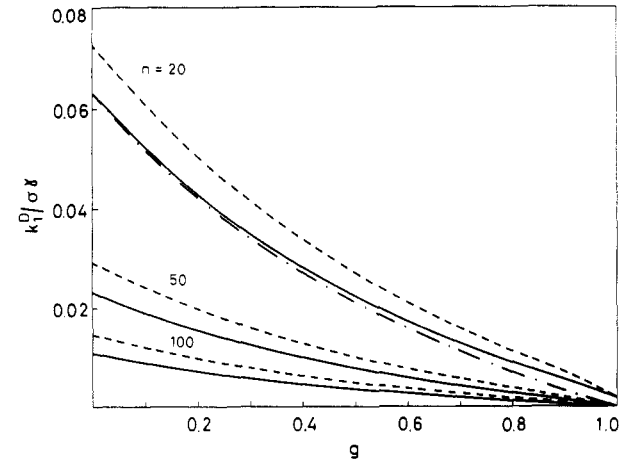

Figure 3. Normalized cyclization rate constant $k_1^{\mathrm{D}}/\sigma\gamma$ as a function of the stiffness parameter g, for $n = 20$, 50, and 100. Full curves, $\gamma_0 = 0.5$; dashed curves, $\gamma_0 = 0.005$. Renormalized Gaussian chain, eq 44, for $\gamma_0 = 0.5$ and $n = 20$: – · –.

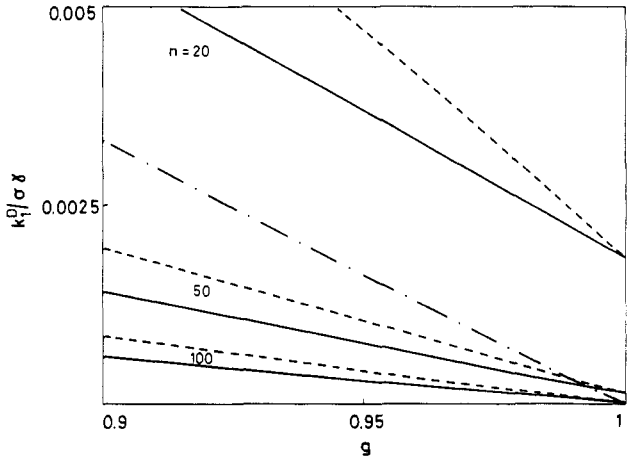

Figure 4. Magnification of Figure 3 in the large stiffness region.

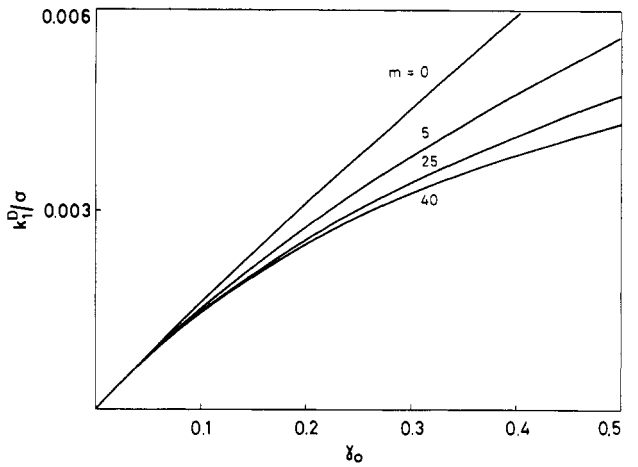

Figure 5. Normalized cyclization rate constant k_1^D/σ for two internal reactive groups separated by $n = 20$ beads and with two equal tails of length m, as a function of the capture strength γ_0. Gaussian chain ($g = 0$). The values of m are reported on the curves.

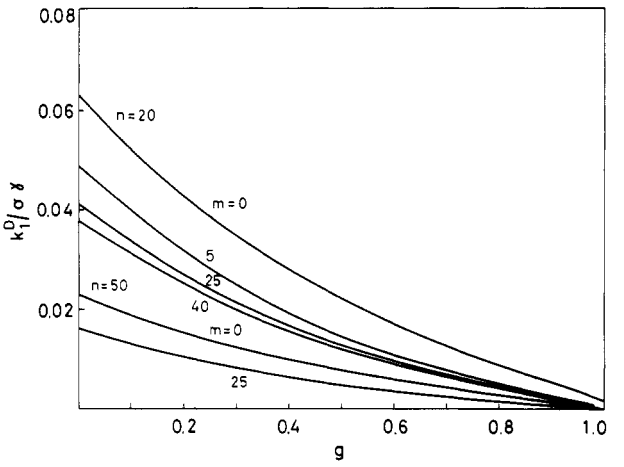

Figure 6. Normalized rate constant $k_1^D/\sigma\gamma$ for two internal reactive groups as a function of the stiffness parameter g at $\gamma_0 = 0.5$: upper curves $n = 20$, the two lower curves $n = 50$. The length of the tails m are reported on the curves.

dependence on the stiffness parameter g, while in the Gaussian limit, k_1^D is given in terms of the number of segments and of segment length l'. For small stiffness, the freely rotating chain reduces to a Gaussian chain with renormalized segment length given by

$$l' = l[(1+g)/(1-g)]^{1/2} \tag{44}$$

This implies the dependence of k_1^D on g:

$$k_1^D(l') = k_1^D(l)[(1-g)/(1+g)]^{3/2} \tag{45}$$

with $k_1^D(l)$ the rate constant for a Gaussian chain of segment length l.

This dependence is only correct for the incipient stiffness dependence as shown in Figure 3. As stiffness increases the two behaviors diverge smoothly as may be appreciated by looking at the dotted–dashed curve for $n = 20$ and $\gamma_0 = 0.5$.

Tail Effect on the Intramolecular Rate Constant

Within the entire hierarchy of ORZ models the intramolecular statistical properties in the static limit are independent of the tails. But what is the effect of the tails on the intramolecular dynamics and particularly on the intramolecular rate constant? In order to simplify the problem, with reference to Figure 1b, let us consider the case of a reactive and a catalytic site in a symmetrical position relative to the center of the chain. With a chain of N beads, a reactive–catalytic site distance of $n - 1$ beads, and two tails of m beads we have

$$N = n + 2m \tag{46}$$

The new parameters of the calculation are now n and m and for $m = 0$ we obtain the end-to-end cyclization case. The effect of increasing the length of the tails on the intramolecular rate constant is described in Figures 5 and 6 for the Gaussian chain ($g = 0$) and for semiflexible chains ($g \neq 0$), respectively. The rate constant decreases asymptotically with increasing length of the tails, and the tail effect increases with the capture strength γ_0 (see Figure 5). Note that in Figure 6, as in Figures 3 and 4, a small nonzero rate constant survives at $g = 1$, showing the failure of the ORZ approximation for the DCR at very high stiffness.

The relative variation of k_1^D with m and n may be better appreciated quantitatively in Table I where the ratios $100[k_1^D(n,m=0) - k_1^D(n,m)]/k_1^D(n,0)$, representing the decrease percentage of the rate constant with the length of the tail, are reported as a function of n and m at several values of γ_0 for $g = 0$. At fixed n the ratios strongly increase with m and with the capture strength γ_0. At small reaction radius the rate decrease percentage is very small and it increases slightly with the distance between the reacting groups but remains nonobservable (for instance for $\gamma_0 \leq 0.05$ the reduction is less than 5%). But at large reaction radius the decrease percentage strongly increases and for $\gamma_0 \geq 0.5$ it is on the order of 40% (although there is a decrease to 30% with increasing distance between the reactive groups). The rate for a tailless chain increases faster with the reaction radius than does the rate for a chain with tails, resulting in this behavior for the relative deviation.

Table I
The Ratio $100[k_1^D(n,m=0) - k_1^D(n,m)]/k_1^D(n,0)$ for a Gaussian Chain[a]

	n		
m	10	20	50
	$\gamma_0 = 0.005$		
10	0.406	0.419	0.433
20	0.447	0.491	0.529
	$\gamma_0 = 0.05$		
10	3.95	4.02	4.37
20	4.58	4.71	4.98
	$\gamma_0 = 0.1$		
10	7.69	7.72	7.41
20	9.11	9.01	8.79
	$\gamma_0 = 0.5$		
10	31.0	27.4	24.4
20	40.7	32.7	28.6

[a] n is the distance between the reactive sites and m is the length of the tails; γ_0 is the capture strength.

For a stiffer chain the tail effect is even larger (see Table II, where the same ratios are reported for $g = 0.6$), having the values of 50% and 40% respectively for $n = 10$ and 50, at $\gamma_0 \simeq 0.5$. Therefore the role of the capture strength is critical for the possibility of observing this tail effect by dynamic experiments. Taking into account that l is on the order of the Gaussian segment length, while R for excimer formation is expected to be on the order of 5 Å, we expect that this dynamic tail effect is better observed the stiffer and shorter the chain. In addition, some dependence on the capture radius should

Table II
The Ratio $100[k_1^D(n,m=0) - k_1^D(n,m)]/k_1^D(n,0)$ for a Semiflexible Chain with Stiffness $g = 0.6$[a]

	n		
m	10	20	50
	$\gamma_0 = 0.005$		
10	0.971	0.962	0.884
20	1.08	1.02	0.980
	$\gamma_0 = 0.050$		
10	8.81	8.49	7.85
20	9.38	9.16	8.78
	$\gamma_0 = 0.1$		
10	15.9	15.1	14.0
20	17.9	16.3	15.4
	$\gamma_0 = 0.5$		
10	44.7	38.7	36.8
20	51.3	44.2	40.4

[a] The same parameters as in Table I.

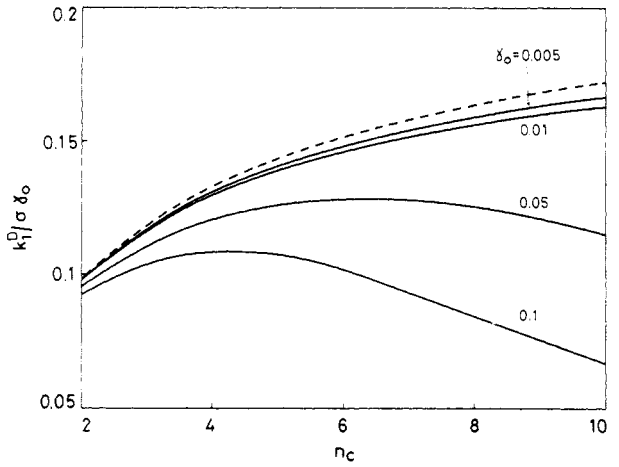

Figure 7. Normalized rate constant $k_1^D/\sigma\gamma_0$ as a function of the number of catalytic sites n_c ($n_b n_c + 1 = n$, the total number of beads). Gaussian chain with a central reactive group and evenly spaced catalytic sites with $n_b = 10$. The values of the capture strength γ_0 are reported on the curves. Dashed curve: the normalized rate constant in the additivity approximation of eq 47, $k_1^{add}/\sigma\gamma_0$ with $c = 0.7536$.

probably be tested by studying intramolecular exciplex formation by couples of different fluorescent groups (of increasing capture radius[6]).

The Reaction Rate Constant for Regularly Spaced Reactive Sites

With reference to Figure 1c let us consider a chain of an odd number n of beads with a reaction group in the middle at position $i_r = (n-1)/2$, containing an even number of catalytic groups n_c spaced by n_b beads with

$$n_b n_c + 1 = n \tag{47}$$

A reaction configuration of this type is realized by a chain containing $n_c + 1$ chromophores regularly distributed with a spacing n_b and with n from (47) very large. With this definition the reaction rate constant is given again by (15) with (30) for $D(t)$. This expression is formally different from the sum of the n_c possible reactions, a form earlier used in the interpretation of excimer formation experiments.[11]

The exact rate constant can be numerically calculated by using (41) with the procedure outlined previously and with a scaling factor τ_p given in Appendix B eq B-1.

In Figure 7, the effects of increasing the number of catalytic sites n_c (and therefore of the molecular weight, according to (47)) is described for a Gaussian chain with a catalytic spacing of $n_b = 10$ for some values of the capture strength. The additivity approximation amounts to

$$k_1^{add} = 2\sum_{p=1}^{n_c/2} k_1^D(pn_b) \simeq \gamma_0 c \sum_{p=1}^{n_c/2} \lambda_1(pn_b) \tag{48}$$

where $k_1^D(pn_b)$ is the diffusion-controlled rate constant for the end-to-end cyclization in a chain with pn_b beads. The last approximation on the right comes from the approximation of $k_1^D(pn_b)$ with its asymptotic expression ($p \gg 1$) evaluated according to eq B-2 in Appendix B, with c a constant value[4] and $\lambda_1(pn_b)$ the first relaxation rate for a chain of pn_b beads. Note that the last expression is simply linear in γ_0. This rate constant is reported as a dashed curve in Figure 7. It clearly appears that only for very small γ_0 does the additivity approximation becomes valid, while for sufficiently high values of γ_0 the rate constant displays first a maximum and then decreases with the further increase of n_c. The smaller γ_0, the higher the number of catalytic sites at which the maximum appears. For large capture strength the dynamic tail effect exerts its depressive action: the greater the capture strength, the stronger the tail effect and the depression of the rate constant. This dynamic depression, in fact, disappears if the total number of beads in the chain is constrained to a constant. In this case, increasing the number of catalytic groups (see Figure 8) increases the rate constant, and this effect is more pronounced the smaller γ_0.

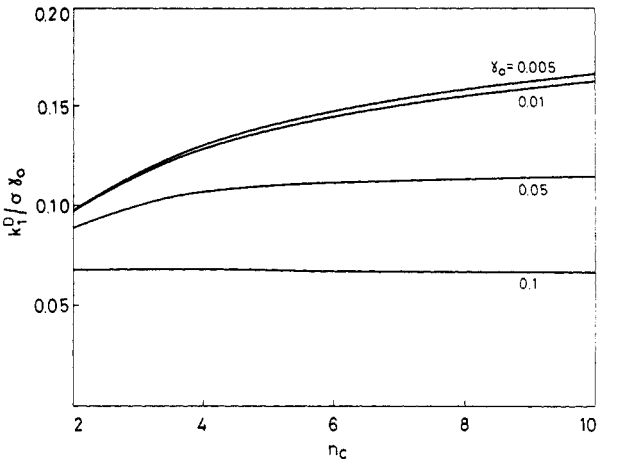

Figure 8. Normalized rate constant $k_1^D/\sigma\gamma_0$ for a Gaussian chain of fixed molecular weight $n = 100$ as a function of the number of the catalytic sites. The catalytic sites are added progressively around the central reactive group with a spacing of $n_b = 10$. The values of the capture strength γ_0 are reported on the curves.

The departure of the rate constant from the additivity limit with increasing number of catalytic groups (and molecular weight) for high values of the capture strength is better appreciated in Figure 9 where the ratio k_1^D/k_1^{add} is reported for a Gaussian chain with $n_b = 5$. Similar plots are obtained for semiflexible chains with $g \neq 0$.

Appendix A. The Sink Function

The sink function describing the region where the reaction between two reactive group can occur is dependent on the distance between the reactive and catalytic groups $\mathbf{R}_{(p)}$. This function with the dimensions of the inverse

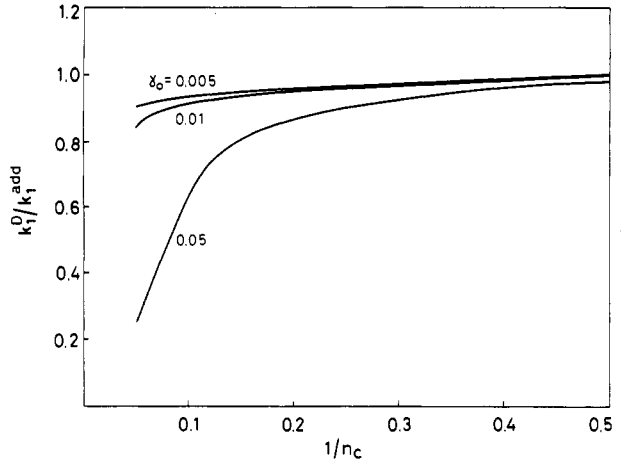

Figure 9. Exact rate constant k_1^D divided by its approximation in the additivity limit, eq 47, as a function of the inverse of the number of catalytic sites $1/n_c$ for a Gaussian chain with catalytic spacing $n_b = 5$ ($n_b n_c + 1 = n$ = total number of beads).

of a volume is chosen normalized in the whole space

$$\int S(\mathbf{R}_{(p)})\, d\mathbf{R}_{(p)} = 1 \qquad \text{(A-1)}$$

Ignoring spatial asymmetries, the sink is assumed spherical

$$S(\mathbf{R}_{(p)}) = S(|\mathbf{R}_{(p)}|) \qquad \text{(A-2)}$$

The simplest sink function is the δ function

$$S(|\mathbf{R}_{(p)}|) = \delta(|\mathbf{R}_{(p)}|) \qquad \text{(A-3)}$$

used to describe a reaction eventually occurring (according to k, see eq 1) at the encounter of the two reacting sites $\mathbf{R}_{(p)} = 0$. Normally the reaction occurs when the reacting groups enter into a finite spatial region, characterized by some radius R. A first description of this type is obtained by a δ function allowing for the reaction to occur at a distance $|\mathbf{R}_{(p)}| = R$:

$$S(|\mathbf{R}_{(p)}|) = \delta(|\mathbf{R}_{(p)}| - R) \qquad \text{(A-4)}$$

A useful approximation to this more complicated sink is obtained by averaging (A-4), $\delta(|\mathbf{R}_{(p)}| - r)$, over a sphere of radius R to obtain the Heaviside sink function

$$S(|\mathbf{R}_{(p)}|) = [(4/3)\pi R^3]^{-1} H(R - |\mathbf{R}_{(p)}|) \qquad \text{(A-5)}$$

with $H(x)$ the Heaviside step function. With this sink the reaction cannot occur outside the sphere of radius R around $|\mathbf{R}_{(p)}| = 0$.

Another computationally useful choice is the Gaussian sink

$$S(|\mathbf{R}_{(p)}|) = (3/2\pi R^2)^{3/2} \exp(-3|\mathbf{R}_{(p)}|^2/2R^2) \qquad \text{(A-6)}$$

All these sinks can be used to describe simple encounter reactions, as in the case of the excimer formation, with very similar results.[17] Note that the sink function can be devised to more properly describe other intramolecular processes. For instance, the electronic excitation energy transfer between two sites on a chain may be described by the sink

$$S(|\mathbf{R}_{(p)}|) = (3/2\pi^2) R_0^3/(R_0^6 + |\mathbf{R}_{(p)}|^6) \qquad \text{(A-7)}$$

according to the $|R_{(p)}|^{-6}$ Forster mechanism with R_0 the distance corresponding to 50% efficiency. Obviously this dependence is expected to give quite different rate constants in comparison to those calculated in this paper by using the sinks (A-3) and (A-5) coupled in an unbalanced choice.

Appendix B. Evaluation of τ_p

According ref 7 and 4 the end-to-end cyclization rate constant can be well approximated for Gaussian chains in nondraining conditions by using

$$\tau_p^{-1} = \gamma_0 6D/L^2\sigma \simeq 0.7536\lambda_1(n)\gamma_0/2 \qquad \text{(B-1)}$$

with D the nondraining translational diffusion coefficient, L^2 the mean square end-to-end distance, and $\lambda_1(n)$ the first relaxation rate for a chain of n beads. When the right-hand side equality in (B-1) is formally extended to the partial draining case ($\zeta_r = 0.25$), the τ_p employed in the computation of equation (41) for both Gaussian and semiflexible chains is obtained. The same expression is assumed to be approximately valid also in the case of a configuration with the reactive groups separated by n beads but with lateral tails of length m. This approximation is insuffcient for high g values: in these cases the procedure is coupled with an ad hoc adjustment of the quadrature intervals. For evenly spaced catalytic sites, k_1^D is estimated from the additivity hypothesis obtaining

$$\tau_p^{-1} \simeq 0.7536\gamma_0 \sum_{i=1}^{n_c/2} \lambda_1(in_b) \qquad \text{(B-2)}$$

where for the end-to-end reaction rate of a chain of length in_b the second relationship in (B-1) is assumed.

References and Notes

(1) Wilemski, G.; Fixman, M. *J. Chem. Phys.* **1973**, *58*, 4009.
(2) Wilemski, G.; Fixman, M. *J. Chem. Phys.* **1974**, *60*, 866.
(3) Wilemski, G.; Fixman, M. *J. Chem. Phys.* **1974**, *60*, 878.
(4) Cuniberti, C.; Perico, A. *Prog. Polym. Sci.* **1984**, *10*, 271.
(5) Cuniberti, C.; Perico, A. *Eur. Polym. J.* **1977**, *13*, 369.
(6) Winnik, M. A. In *Photophysical and Photochemical Tools in Polymer Science*; Winnik, M. A., Ed.; Nato ASI Ser.; Reidel: Dordrecht, 1986; pp 293, 324.
(7) Perico, A.; Cuniberti, C. *J. Polym. Sci., Polym. Phys. Ed.* **1977**, *15*, 1435.
(8) Winnik, M. A.; Redpath, A. E.; Richards, D. H. *Macromolecules* **1980**, *13*, 328.
(9) Redpath, A. E.; Winnik, M. A. *J. Am. Chem. Soc.* **1980**, *102*, 6869.
(10) Cuniberti, C.; Perico, A. *Eur. Polym. J.* **1980**, *16*, 887.
(11) Cuniberti, C.; Perico, A. *Ann. N. Y. Acad. Sci.* **1981**, *366*, 35.
(12) Cuniberti, C.; Musi, L.; Perico, A. *J. Polym. Sci., Polym. Lett. Ed.* **1982**, *20*, 265.
(13) Redpath, A. E.; Winnik, M. A. *Polymers* **1983**, *24*, 1286.
(14) Winnik, M. A.; Li, X. B.; Guillet, J. E. *Macromolecules* **1984**, *17*, 699.
(15) Bixon, M.; Zwanzig, R. *J. Chem. Phys.* **1978**, *68*, 1896.
(16) Morse, P. M.; Feshbach, H. *Methods of Theoretical Physics*; McGraw-Hill: New York, 1953; p 860, eq 7.4.9.
(17) Battezzati, M.; Perico, A. *J. Chem. Phys.* **1981**, *74*, 4527.
(18) Perico, A.; Battezzati, M. *J. Chem. Phys.* **1981**, *75*, 4430.
(19) Wang, M. C.; Uhlenbeck, G. E. *Rev. Mod. Phys.* **1945**, *17*, 323.
(20) Perico, A.; Guenza, M. *J. Chem. Phys.* **1985**, *83*, 3103.
(21) Perico, A.; Ganazzoli, F.; Allegra, G. *J. Chem. Phys.* **1987**, *87*, 3677.
(22) Perico, A.; Bisio, S.; Cuniberti, C. *Macromolecules* **1984**, *17*, 2686.